ACS ES&T Water

Open Access



pubs.acs.org/estwater

Article

# Molecular Alterations of Algal Organic Matter in Oxidation Processes: Implications to the Formation of Disinfection Products

Chao Liu,* Hang Liu, Chengzhi Hu, Alex T. Chow, and Tanju Karanfil*

Cite This: *ACS EST Water* 2024, 4, 5890−5901

Read Online

ACCESS | Metrics & More | Article Recommendations | Supporting Information

**ABSTRACT:** Seasonal algal blooms in surface waters can adversely impact drinking water quality. Oxidative treatment has been demonstrated as an effective measure for the removal of algal cells. However, this, in turn, leads to the release of algal organic matter (AOM). Effects of oxidative treatment using chlorine, bromine, chloramine, ozone, and permanganate on the molecular alterations of the AOM were studied using Fourier transform ion cyclotron resonance mass spectrometry. Increased chemodiversity, decreased aromaticity, and elevated average oxidation state of carbon ($\overline{OS_c}$) were observed after oxidation. Of the oxidants, ozone caused the most pronounced changes. There was a positive correlation between the increases in $\overline{OS_c}$ and reduction potentials of oxidants (i.e., ozone > chlorine ≈ bromine > permanganate > chloramine). Oxygen transfer and oxidative dehydrogenation were major pathways (42.3−52.8%) for AOM oxidation, while other pathways (e.g., deamination, dealkylation, decarboxylation, and halogen substitution/addition) existed. Moreover, the halogen substitution/addition pathway only accounted for 1.3−10.3%, even for chlorine or bromine treatment. Oxidative treatment could decrease the reactivity of AOM in postchlorination, thereby decreasing the trichloromethane formation. However, the formation of oxygen-rich disinfection byproducts (DBPs, e.g., trichloronitromethane) could be favored, especially for ozonation. This study provides molecular-level insights into the effects of oxidative treatment on AOM and derived DBP formation in water treatment.

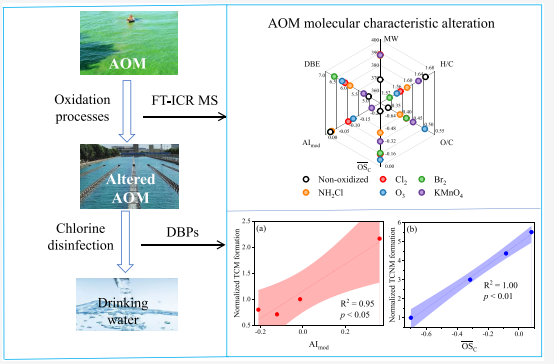


**KEYWORDS:** *algal organic matter, FT-ICR MS, ozonation, bromination, chloramination, permanganate, chlorination, disinfection byproducts*

## INTRODUCTION

The increasing occurrence of harmful algal blooms (HABs) in lakes and reservoirs worldwide has posed grave threats to both public health and aquatic ecosystems.[1] Owing to global warming, eutrophication, wildfire, and increasing $CO_2$ levels, the frequency, duration, and intensity of HABs have risen.[2−5] Algae cells in surface water seasonally proliferate, releasing bulk algal organic matter (AOM) and trace amounts of metabolites (e.g., toxins, taste, and odor compounds), which can cause adverse impacts on drinking water quality.[6−8]

During seasonal algal bloom events, oxidative treatment using representative oxidants (e.g., chlorine, ozone, and permanganate) ahead of the conventional process has been demonstrated as an effective measure for the enhanced abatement of algal cells by conventional coagulation process.[9−14] For example, chlorine can be occasionally spiked at the source water intake points to improve algae removal.[9] The mechanisms for the algae removal improvement include cell external morphology change, release of cell-derived polymeric material behaving as a coagulant aid, and degradation of AOM.[10]

While oxidative treatment can be beneficial for enhanced algae removal, oxidants can destroy algae cells and lead to the release of AOM into the treated waters.[9,15,16] AOM is composed of lipid, carbohydrate, protein, and nucleic acid, showing hydrophilic character and low-specific UV absorbance (SUVA) values (<2.0 L $mg^{-1}$ $m^{-1}$).[17,18] This is in contrast to terrestrial natural organic matter (NOM), which is characterized by polyphenolic types of structure.[19] In oxidative treatment processes, oxidants can react with the released AOM and thereafter alter its chemical composition. Chlorine reacts with organics through halogen substitution and electron transfer pathways.[20] The former can lead to the formation of chlorinated disinfection byproducts (DBPs),[6,16,21,22] while the latter pathway yields an oxidized form of AOM. Common reaction pathways of ozone and permanganate with organics

Received: September 9, 2024
Revised: November 14, 2024
Accepted: November 15, 2024
Published: November 25, 2024

include addition and electron transfer.[23] Ozone is a stronger oxidant than permanganate. In addition, OH radicals, being the strongest oxidants in water, can be formed due to ozone decomposition. In addition, naturally occurring bromide and ammonia can react with oxidants (e.g., chlorine) to produce secondary oxidants (i.e., hypobromous acid (HOBr) and chloramines, respectively),[24] which are expected to react with AOM via halogen substitution and electron transfer pathways. Our previous studies showed that HOBr reacts more readily with dissolved organic matter (DOM) with low SUVA (e.g., AOM), yielding high amounts of halogenated DBPs. Yet, chlorine preferentially reacts with NOM over AOM.[21,25] This indicates that the transformation of DOM and formation of byproducts depend on the type of oxidants employed and the characteristics of DOM.

To unravel the transformation of NOM at the molecular level in various oxidation processes, the application of Fourier transform ion cyclotron resonance mass spectrometry (FT-ICR MS) has been widely implemented owing to its ultrahigh resolving power and mass accuracy.[26−32] Based on the exact molecular formulas of products using FT-ICR MS, it was found that there were fewer aromatic precursors from AOM than NOM.[33] Chlorination of AOM led to the diversification of nitrogenous molecular formulas due to the breakdown of larger peptides and the formation of chloramine-type functional groups.[33] On the contrary, ozone can increase the O/C and decrease H/C ratios of the assigned formulas in AOM, which decreases the formation of trichloromethane in postchlorination.[34] This indicates a distinct reaction pathway for ozonation compared with chlorination. As mentioned above, various oxidants, such as chlorine, ozone, and permanganate, have been used in HAB events. However, the effects of oxidative treatment with these oxidants and secondarily formed bromines and chloramines on the molecular transformation of AOM remain largely unknown. The underlying mechanisms will help to predict the formation of toxic DBPs in the subsequent chlorine disinfection process.

Given the increasing occurrence of HAB events in lakes and reservoirs worldwide, this study aims to (1) elucidate the alteration of molecular compositions and properties of AOM during oxidation processes using chlorine, bromine, chloramine, ozone, and permanganate, (2) study the formation pathways of unknown products during oxidative treatment of AOM, and (3) develop the relationship between AOM molecular characteristics and DBP formation upon subsequent chlorine disinfection.

## MATERIALS AND METHODS

**Reagents.** Chlorine stock solutions (5% active chlorine) were provided by J.T. Baker. Stock solutions of bromine were freshly prepared by the reaction of bromide and hypochlorite at a molar ratio of 1.05.[25] Monochloramine stock solutions were prepared by the dropwise addition of hypochlorite to the solutions of ammonium chloride ($NH_4Cl$) at a molar $Cl_2$/N ratio of 0.2 at pH 8.8. Solutions of ozone (~30 mg $L^{-1}$) were freshly prepared by bubbling ozone gas to the deionized Milli-Q water (18.2 MΩ·cm) with an oxygen-fed ozone generator (GTC-1B, Griffin Technics Inc.).

In this study, AOM was extracted from *Microcystis aeruginosa*, which was selected to be the model algae strain due to its wide occurrence during HAB events in lakes and reservoirs.[22] The algae culturing and AOM extraction procedures were adapted from the literature[21] (see details in the Supporting Information, Text S1). The dissolved organic carbon (DOC) and dissolved organic nitrogen (DON) of AOM solutions used in this study were 2.0 and 0.35 mg $L^{-1}$, respectively, with a SUVA of 1.5 L $mg^{-1}$ $m^{-1}$.

**Experiments for Oxidation of AOM.** For oxidation of AOM, experiments were carried out in ~1 L bottles at room temperature (21 ± 1 °C). Solutions of oxidants (e.g., chlorine, bromine, preformed chloramine, ozone, and permanganate) were injected into the AOM solutions (pH 7.5, 5 mM phosphate buffer) to initiate the reactions. The initial oxidant concentration was 4 mg $L^{-1}$ as $Cl_2$ for a contact time of 0.5−24 h (except for ozone, 2 mg $L^{-1}$ for 10 min due to its rapid decay). The contact time was selected because in cases when oxidants are applied at the intake points before delivering the water to treatment plants,[9] a long oxidation time (up to >10 h) can be required. After the oxidation treatment, samples were quenched by sodium sulfite. Analytical methods for various oxidants are detailed in Text S2.

**Water Sample Enrichment.** The organics resulting from oxidized AOM were concentrated by solid-phase extraction (SPE) based on a previous study,[35] which has been widely used to extract AOM for FT-ICR MS analyses.[33,36] One AOM sample without oxidative treatment was used as the control. The styrene−divinylbenzene polymer (Bond Elut-PPL, 1 g, Agilent) cartridges were preconditioned with 3 mL of methanol. Prior to SPE, water samples were adjusted to pH 2 by 6 M hydrochlorous acid, and then, they were loaded to SPE cartridges at a flow rate of ~5 mL $min^{-1}$. Afterward, all cartridges were washed with 10 mL of 0.1% formic acid solutions. Once washed, cartridges were dried with $N_2$ gas and eluted with 3 mL of methanol. The methanol extract was then reduced to 1 mL by $N_2$ gas blow-down. All extracts were stored at −20 °C prior to MS analyses. It should be noted that there were certain limitations to the sample enrichment processes. We were able to analyze only the adsorbed AOM fractions on the PPL cartridge in this study.

**FT-ICR MS.** The SPE extracts of AOM solutions were diluted 100 times with methanol and injected into a 12 T Bruker SolariX FT-ICR MS instrument at the Pacific Northwest National Laboratory, WA, using negative mode electrospray ionization. The mass range for the sample measurement was at $m/z$ of 100−1000 Da and after internal calibration, the deviation for mass measurement was less than 1 ppm. To process the data, a MS peak picker with an intensity threshold of 100 and a signal-to-noise threshold of 7 was employed.[37]

Assignment for molecular formulas was performed with element combinations of $^{12}C_{1-60}$, $^{13}C_{0-1}$, $^{1}H_{1-120}$, $^{16}O_{1-50}$, $^{14}N_{0-5}$, $^{32}S_{0-2}$, $^{31}P_{0-2}$, $^{35}Cl_{0-3}$, $^{37}Cl_{0-1}$, $^{79}Br_{0-3}$, $^{81}Br_{0-1}$ and criteria of H/C < 2.2 and O/C < 1.2 using an in-house written python script.[38,39] For the equivocal peaks that were assigned to multiple formulas (mass error <0.5 ppm), the optimum formula was selected based on patterns of homologous series and the lowest numbers of heteroatoms. The numbers of chlorine and bromine were verified based on characteristic isotopic patterns.

**Data Analyses.** Based on the element compositions of the assigned formulas ($C_cH_hO_oN_nP_pS_sX_x$, X represents Cl or Br) of nonoxidized and oxidized AOM, the average oxidation state of carbon ($\overline{OS_c}$) can be calculated according to eq 1 with modifications on a previous study.[40]



https://doi.org/10.1021/acsestwater.4c00855
ACS EST Water 2024, 4, 5890−5901

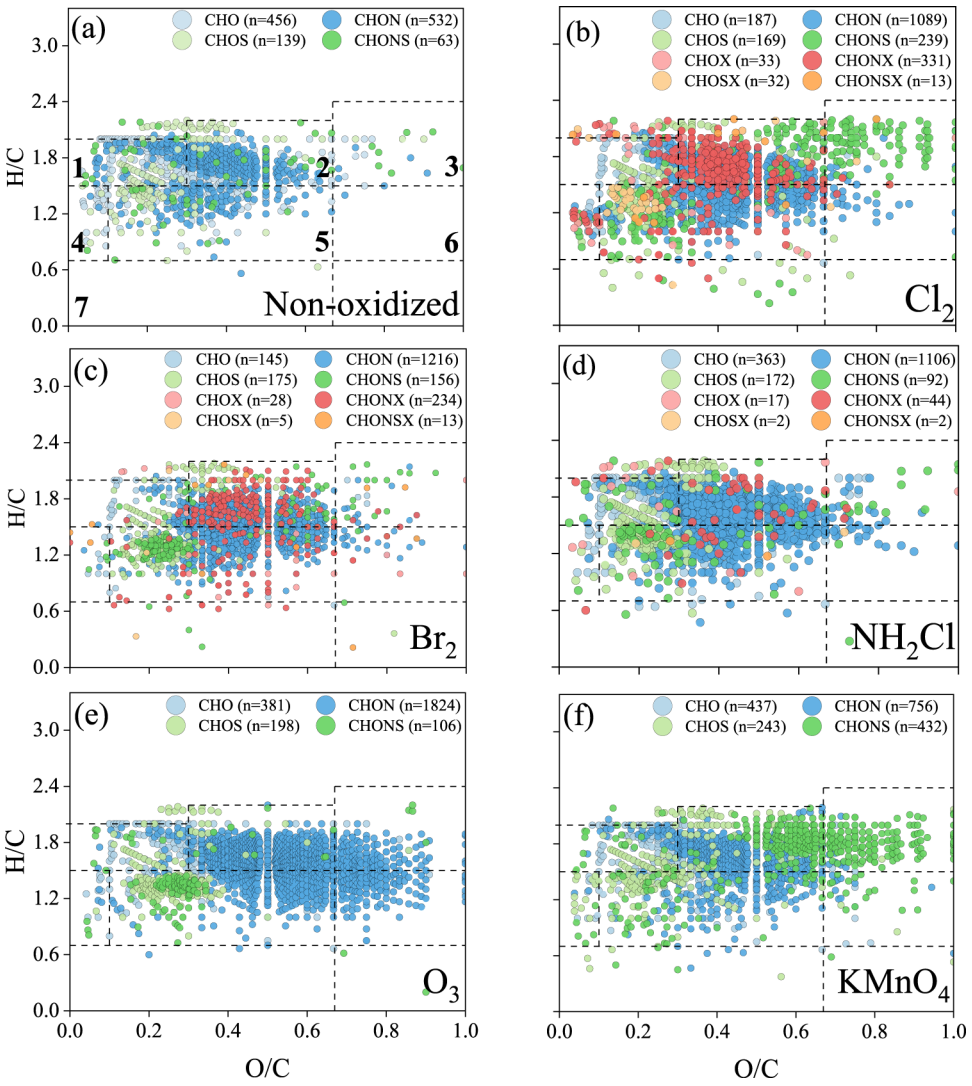


**Figure 1.** Van Krevelen diagrams of AOM without oxidation treatment (a) and treated with (b) chlorine, (c) bromine, (d) chloramine, (e) ozone, and (f) permanganate. The regions indicate (1) lipids, (2) aliphatic/peptides, (3) carbohydrates, (4) unsaturated hydrocarbons, (5) lignin/CRAM (carboxylic-rich aromatic moieties)-like, (6) tannins, and (7) aromatic structures, respectively, based on the literature.[42]

$$\overline{OS_c} = 4 - \frac{4c + h - x - 3n - 2o - 2s + 5p}{c} \quad (1)$$

Other molecular parameters including modified aromaticity index ($AI_{mod}$), double-bond equivalent (DBE), DBE/C, DBE/O, DBE-O, (DBE-O)/C, and number-averaged values of molecular weight (MW) were calculated based on element compositions, which are detailed in Text S3. The Kendrick mass defect (KMD) analyses were also carried out to show the chemodiversity of possible precursor-product pairs.[41] The equations of KMD calculation can be found in Text S3.

In the van Krevelen (VK) diagram, assigned formulas were categorized into various regions using the boundary limits as summarized in Table S1.[42] Plot of (DBE-O)/C vs $\overline{OS_c}$ was applied for the visualization of the saturability and carbon oxidation state of assigned formulas (Table S2). In addition, the categorization of assigned formulas was based on the boundary limits of the $AI_{mod}$ and H/C values (Table S3). Based on their occurrence, the assigned formulas were classified into three groups: (1) formulas abated upon oxidation, (2) formulas resistant in relative intensity (−0.5−2.0), and (3) formulas formed upon oxidation. It should be noted that formulas reacted might be classified as resistant formulas with this classification approach.

To reveal the transformation pathways during oxidation processes, mass difference network analyses were conducted using possible precursor-product pairs, which were visualized by the open-source Gephi software. Analyses were performed based on seven types of reactions (i.e., oxygen transfer, oxidative dehydrogenation, deamination, dealkylation, decarboxylation, chlorine/bromine substitution, and chlorine/bromine addition), as detailed in Table S4. For the comparison between each pair of groups, the statistical analysis was conducted with one-way analysis of variance (ANOVA).

## RESULTS AND DISCUSSION

**Alterations of AOM Molecular Characteristics in Oxidation Processes.** The VK diagrams reveal the distribution of assigned formulas with lipids, aliphatic/peptides, carbohydrates, unsaturated hydrocarbons, lignin/carboxylic-rich aromatic moieties (CRAMs), tannins, and aromatic structures (Figures 1 and S1). Figure S2 illustrates the distribution of assigned formulas in the plot of (DBE-O)/


https://doi.org/10.1021/acsestwater.4c00855
ACS EST Water 2024, 4, 5890−5901

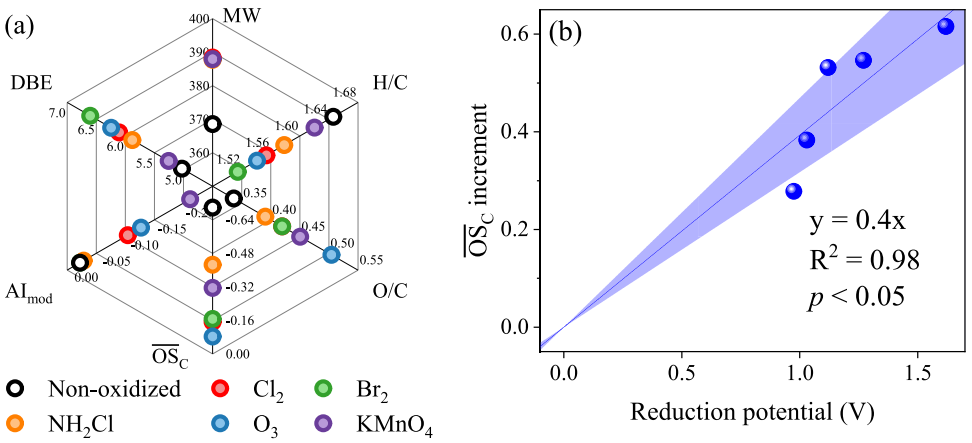


**Figure 2.** Molecular characteristics of assigned formulas in nonoxidized AOM and treated with chlorine, bromine, chloramine, ozone, and permanganate (a) and the relationship between $\overline{OS}_c$ increment and reduction potentials of oxidants (pH 7.5, 25 °C) (b). The data on the reduction potentials of oxidants were from the literature.[48]

C vs $\overline{OS}_c$, in which the regions I, II, III, and IV indicate unsaturated and oxidized compounds, unsaturated and reduced compounds, saturated and reduced compounds, and saturated and oxidized compounds, respectively. Changes of molecular parameters, including MW, H/C, O/C, $\overline{OS}_c$, AI$_{mod}$, and DBE of AOM upon oxidation, are shown in Figures 2 and S3.

As shown in Figure 1, large amounts of nitrogen-containing formulas (i.e., CHON and CHONS molecules) were assigned in the AOM, accounting for 51.8% of the total formulas assigned. Approximately 90% of the AOM formulas with ratios of O/C (0.03−0.60) and H/C (1.20−2.20) fell into the regions of lipids, aliphatic/peptides, unsaturated hydrocarbons, and lignin/CRAM. These findings revealed the substantially distinct molecular characteristics of AOM as compared to Suwannee River (SR) NOM (Figure S1). CHO molecules predominated in NOM with a fraction of 79.9%, and the assigned formulas were mainly characterized as lignin/CRAM-like and tannin structures. The distribution of assigned formulas agrees well with the nature of AOM since AOM contains amino acids/proteins, carbohydrates, nucleic acids, and lipids.[25] The number-averaged values of O/C, H/C, $\overline{OS}_c$, DBE, and AI$_{mod}$ of AOM were 0.34, 1.65, −0.70, 5.03, and −0.01, while the values of their counterparts of NOM were 0.54, 1.03, 0.08, 11.39, and 0.36, respectively. As summarized in Table S5, in addition to the previously reported low aromaticity of AOM,[6] the molecular-level parameters further indicated the lower $\overline{OS}_c$ and higher degree of saturation of AOM as compared to various types of DOM including SR NOM and forest-sourced water.[43] The plot of (DBE-O)/C vs $\overline{OS}_c$ in AOM also revealed that assigned formulas were in the regions of low $\overline{OS}_c$. Based on AI$_{mod}$ and H/C values, aliphatic structures accounted for 64.9% of the total assigned AOM formulas. Yet, the fraction of highly unsaturated and phenolic structures was 23.1%. It is noted that 82.9% of the assigned formulas of NOM belonged to highly unsaturated and phenolic structures.

Oxidation processes largely changed the molecular characteristics of AOM (Figures 1 and 2). 1190 formulas were identified in the nonoxidized AOM samples. The total numbers of assigned formulas, however, were 2093, 1962, 1818, 2509, and 1868 after chlorination, bromination, chloramination, ozonation, and permanganate treatment, respectively. In chlorination and bromination, the average values of MW increased from 368.57 to 388.40 and 406.87 Da, respectively, which could be ascribed to the incorporation of chlorine/bromine.[44] In agreement with the distribution of assigned AOM formulas, the chlorine/bromine-containing formulas were mainly characterized as aliphatic/peptides and lignin/CRAM-like structures by VK diagrams. Meanwhile, the $\overline{OS}_c$ increased from −0.70 to −0.19 due to the electron transfer pathway in chlorination/bromination. VK diagrams and plot of (DBE-O)/C vs $\overline{OS}_c$ also revealed the formation of formulas with increased $\overline{OS}_c$ in chlorination/bromination. Given that chloramine is a weak oxidant,[45] changes in AOM characteristics were obviously less pronounced in chloramination than in chlorination and bromination. For example, the average $\overline{OS}_c$ slightly increased from −0.70 to −0.43 upon chloramination.

Owing to the strong oxidation capacity of ozone, substantial amounts of formulas in regions of aliphatic/peptides, carbohydrates, lignin/CRAM-like, and tannins with high O/C values were observed upon ozonation. Over 1000 saturated and oxidized products were assigned in ozonated AOM, in contrast to <100 in nonoxidized AOM (Figure S2). Ozone was reactive toward activated aromatic compounds, double bonds, and nonprotonated amines,[46] leading to the substantially decreased AI$_{mod}$ and (DBE-O)/C values in ozonated AOM. As revealed in Figure S3, the distribution of O/C values of formulas obviously moved toward high O/C regions upon ozonation.

Permanganate oxidation increased the number of formulas detected. Compared with other oxidation processes, high amounts of sulfur-containing formulas were observed upon permanganate oxidation (Figure 1). It was reported that permanganate can preferentially oxidize aromatic nitrogen-containing components,[47] decreasing the aromaticity of AOM (i.e., AI$_{mod}$). This reaction could lead to the formation of aliphatic nitrogen and benzoic acid with cleavage of a nitrogen-containing group from the aromatic ring, which probably contributed to the abundant CHON and CHONS molecules in the region of aliphatic/peptides and carbohydrates in VK diagrams. In addition, the permanganate-induced changes in molecular characteristics were less pronounced than those of ozone, agreeing well with a previous study on the MW


https://doi.org/10.1021/acsestwater.4c00855
ACS EST Water 2024, 4, 5890−5901

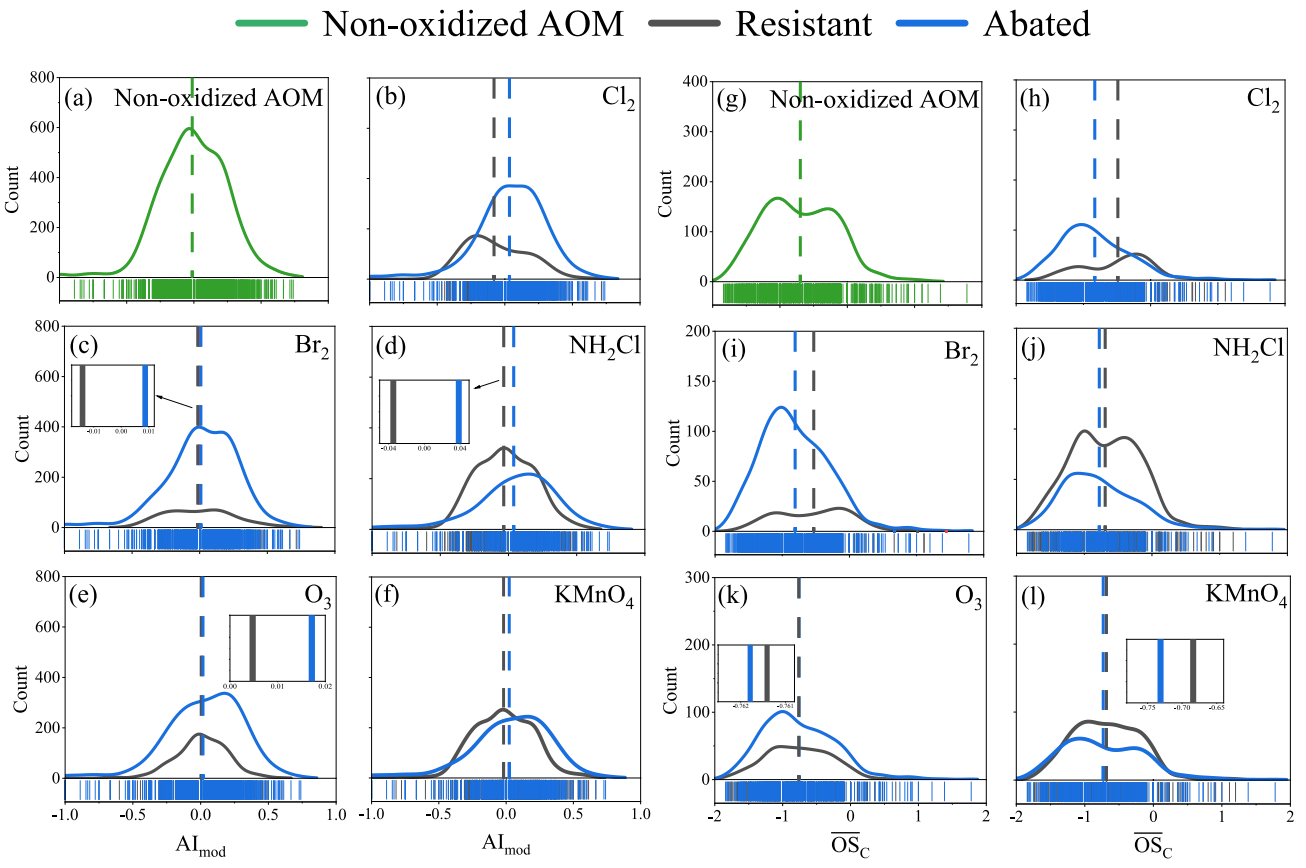


**Figure 3.** Comparison of (a–f) $AI_{mod}$ and (g–l) $\overline{OS}_c$ values of formulas that are resistant and abated in (a and g) nonoxidized AOM and treated with (b and h) chlorine, (c and i) bromine, (d and j) chloramine, (e and k) ozone, and (f and l) permanganate. Dashed lines indicate the average values of formulas that are present in nonoxidized AOM (green), resistant (dark gray), and abated (blue).

distribution and fluorescence characteristics of AOM upon ozonation and permanganate treatment.[15]

Among the five oxidation processes, the most substantial elevation in $\overline{OS}_c$ of AOM was observed upon ozonation, as indicated by the increased O/C and $\overline{OS}_c$ values (Figures 2 and S3). A positive relationship was established between $\overline{OS}_c$ increments and reduction potentials of oxidants (i.e., ozone > chlorine ≈ bromine > permanganate > chloramine).[48] Meanwhile, treatment with permanganate and ozone obviously decreased the aromaticity of the AOM. A more pronounced reduction was observed in ozonation compared to permanganate treatment since ozone and its secondarily formed products (e.g., OH radicals) are stronger oxidants than permanganate. In contrast, the aromaticity remained nearly unchanged upon bromination and chloramination. All of the five oxidation processes increased the average DBE values of AOM. The changes in DBE/C, DBE/O, and DBE-O further revealed that C═C unsaturation contributed to the increased DBE of AOM upon chlorination and chloramination, while C═O bonds drove the DBE increase of AOM treatment with ozone and permanganate (Table S6).

**Formulas Susceptible to Oxidation Processes.** To further understand the transformation of AOM, formulas susceptible to oxidation (i.e., abated) are compared with those resistant to oxidation (Figures 3 and S4–S6). The numbers of abated formulas were 624, 589, 358, 596, and 426 in chlorination, bromination, chloramination, ozonation, and permanganate oxidation, respectively, accounting for 52.4, 49.5, 30.1, 50.1, and 35.8% of the total assigned formulas in nonoxidized AOM (Figure S4). Meanwhile, approximately 24.4, 23.3, 53.4, 25.9, and 46.6% of the assigned formulas remained resistant. These findings confirm the higher reactivity of chlorine, bromine, and ozone toward AOM than chloramine and permanganate. Approximately 45.8 to 74.7% of the highly unsaturated and phenolic structures in AOM were removed upon oxidation, while the percentages of aliphatic structures that were abated ranged from 23.6 to 57.6% (Figure S5).

In chlorination, significantly lower $\overline{OS}_c$ and higher $AI_{mod}$ values of abated formulas were observed as compared to the resistant formulas (Figures 3 and S4), indicating the reactivity of compounds with relatively low $\overline{OS}_c$ and high aromaticity toward chlorine. Over 70% of the highly unsaturated and phenolic compounds in AOM were abated (Figure S5), agreeing well with the previous finding that the phenolic group was the reactive site for chlorine.[49]

In consistency with chlorination, approximately 70% of highly unsaturated and phenolic compounds in AOM were abated upon bromination. Meanwhile, 57.6% of aliphatic compounds were abated in bromination, which was 1.3 times as high as those in chlorination (Figure S5). This agreed well with our previous findings that HOBr has a higher reactivity with aliphatic moieties in AOM than HOCl.[22] Thus, no significant difference was observed between the $AI_{mod}$ values of the resistant and abated formulas during AOM bromination (Figures 3 and S6). In line with chlorination, $\overline{OS}_c$ values of


https://doi.org/10.1021/acsestwater.4c00855
ACS EST Water 2024, 4, 5890–5901

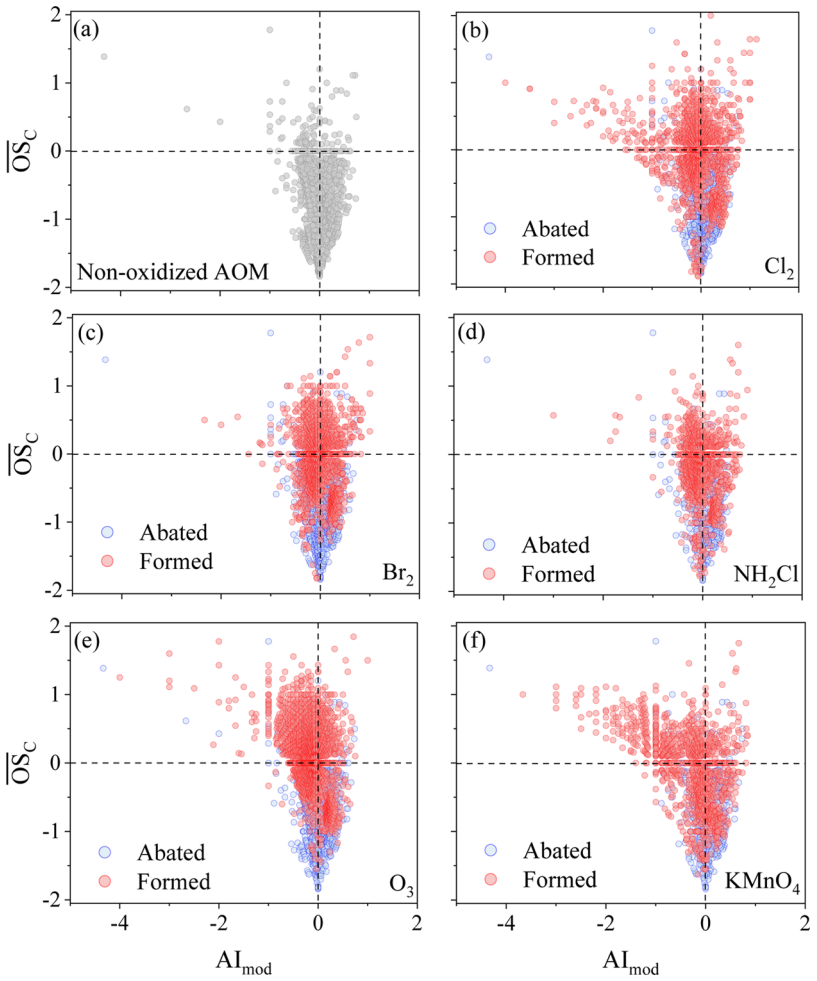


**Figure 4.** Distribution of formulas that are (a) present in nonoxidized AOM, (b–f) abated, and formed in AOM treated with (b) chlorine, (c) bromine, (d) chloramine, (e) ozone, and (f) permanganate in the plot of $AI_{mod}$ vs $\overline{OS_c}$.

abated formulas were significantly lower than those of resistant formulas.

Only 30.1% of the assigned formulas in AOM were abated due to the low reactivity of chloramine, while >53.4% persisted in chloramination (Figure S4). The abated formulas in chloramination were characterized with significantly lower $\overline{OS_c}$ and higher $AI_{mod}$ than those of the resistant formulas (Figure 3). Additionally, the average DBE value of abated formulas was significantly higher than the resistant formulas, which could be ascribed to the nucleophilic addition of chloramine.[50]

In ozonation, nearly 600 formulas were abated, accounting for 50.1% of the total assigned formulas in the AOM (Figure S4). Higher levels of CHON molecules were abated upon ozonation than chlorination and chloramination (267 versus 116–203). Compared to the resistant CHON formulas in ozonation, abated CHON formulas were characterized by low O/C values (0.31 vs 0.40), high DBE values (5.61 vs 5.31), and high $AI_{mod}$ (0.01 vs −0.16). Meanwhile, highly unsaturated and phenolic compounds accounted for 36.9% of the total abated formulas, while for aliphatic compounds, it was 56.0% (Figure S5). However, both the $AI_{mod}$ and $\overline{OS_c}$ values showed no significant differences between the abated and resistant formulas (Figures 3 and S6).

In permanganate treatment, ∼35.8% of the assigned formulas in AOM were abated, while 46.6% of the assigned formulas persisted, indicating again its relatively lower reactivity toward AOM than ozone (Figure S4). The number-averaged $AI_{mod}$ of resistant formulas was slightly lower than that of removed formulas upon permanganate oxidation (Figures 3 and S6), which could imply the higher reactivity of permanganate toward aromatic compounds than aliphatic compounds.[51]

Overall, the number-averaged $AI_{mod}$ values of abated formulas were significantly higher than those of resistant formulas in chlorination and chloramination, while no significant difference was observed in bromination and ozonation. Meanwhile, the abated formulas in chlorination, bromination, and chloramination were characterized as low $\overline{OS_c}$ than the resistant formulas, while similar $\overline{OS_c}$ values of abated and resistant formulas were observed in ozonation and permanganate treatment. These results indicated that the components with high aromaticity and low $\overline{OS_c}$ were prone to oxidation process.

**Formulas Formed after Oxidation Processes.** Figures 4 and S6 compare the molecular characteristics of formed and abated formulas. The VK diagrams of formulas upon oxidation are shown in Figures S7–S9. The KMD plots are applied to reflect the chemodiversity of formulas (Figure S10). Approximately 1000 to 2000 formulas were formed in the five oxidation processes, which were 2.1–3.2 times as high as those of the abated formulas in each process. This is not



https://doi.org/10.1021/acsestwater.4c00855
ACS EST Water 2024, 4, 5890–5901

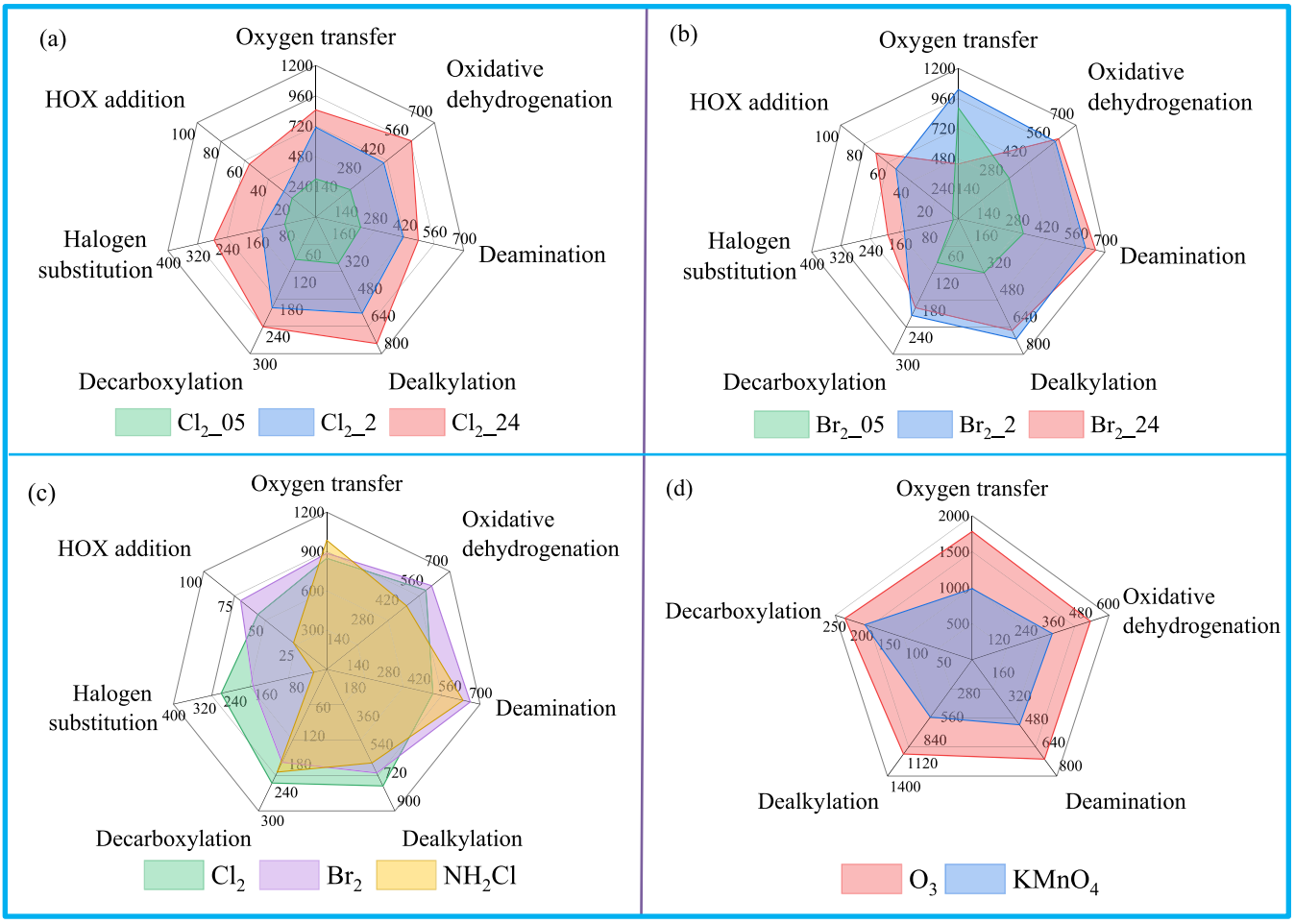


**Figure 5.** Number of possible precursor-product pairs identified between formulas in nonoxidized AOM and products in oxidation processes: (a) 0.5, 2, and 24 h chlorination; (b) 0.5, 2, and 24 h bromination; (c) chlorination, bromination, and chloramination; and (d) ozonation and permanganate oxidation.

surprising since numerous transformation products can be formed from one precursor via various pathways. In addition, the amounts of nitrogen-containing formulas were 2.3−7.0 times higher than those without nitrogen, which could be ascribed to the high nitrogen content in AOM.

A total of 411 chlorine-containing formulas were formed in the chlorination process, which were mainly in the aliphatic/peptide-like region. Among them, the numbers of formulas containing one (i.e., CHOCl and CHONCl), two (i.e., $CHOCl_2$ and $CHONCl_2$), and three chlorine atoms (i.e., $CHOCl_3$ and $CHONCl_3$) were 210, 153, and 48, respectively (Figure S7). In addition, out of the 411 formulas, >83.7% contained nitrogen (i.e., $CHONCl_{1-3}$ and $CHONSCl_{1-3}$). Since nitrogen-containing formulas contributed to 50% of the nonoxidized AOM pool, this indicated the high potential of CHON groups to form chlorinated byproducts, probably organic chloramines.[52] Furthermore, 1108 formed formulas did not contain chlorine atoms, mainly in the aliphatic/peptide-like and lignin/CRAM-like regions. Decreased $AI_{mod}$ and increased $\overline{OS}_c$ were observed in formed formulas during chlorination of AOM (Figure 4).

In bromination, 283 bromine-containing formulas were formed (Figure S7). Formulas containing one or two bromine atoms predominate, and those containing three bromine atoms were not detected. The instability of brominated byproducts could be the cause.[21,53] Akin to chlorination, 84.4−88.4% of these formulas also contained nitrogen atoms. Though larger amounts of assigned formulas in AOM were abated in bromination than chlorination, the numbers of bromine-containing formulas were lower than those in their chlorinated analogues. In contrast to chlorination, no significant difference was observed between the $AI_{mod}$ of abated and formed formulas (Figures 4 and S6).

A total of 986 formulas were formed in the chloramination of AOM, which were obviously lower than those in chlorination and bromination. Among them, ∼93.2% did not contain chlorine atoms (Figure S8), indicating the minor contribution of the halogen substitution pathway in chloramine treatment.

In ozonation, 1915 formulas were formed, which were 2.2 times higher than those of the abated formulas. As illustrated in Figure S9, the distribution of transformation products in VK diagrams dramatically moved toward the high O/C regions. The average values of O/C and $\overline{OS}_c$ increased from 0.30 and −0.76 in the abated formulas to 0.55 and 0.09 in the formed formulas (Figures 4 and S6), respectively, agreeing well with a previous study.[34] Due to the strong oxidation capacity of ozonation, the O/C and $\overline{OS}_c$ values of formulas formed in ozonation were significantly higher than other oxidation processes. For example, negative average $\overline{OS}_c$ values (i.e.,


https://doi.org/10.1021/acsestwater.4c00855
ACS EST Water 2024, 4, 5890−5901

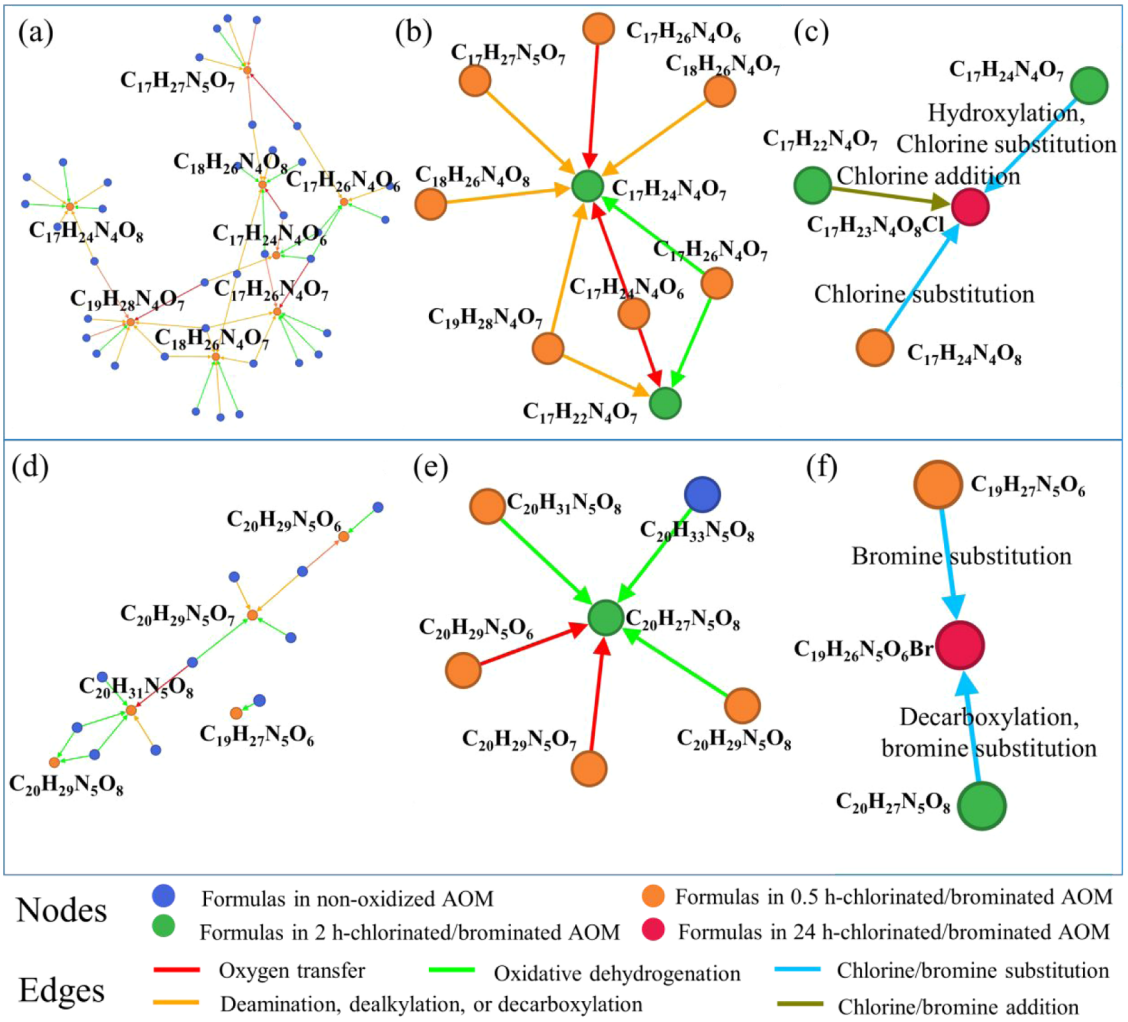


**Figure 6.** Mass difference network analysis showing the reactions for the formation of $C_{17}H_{23}N_4O_8Cl$ in chlorination (a: 0−0.5 h; b: 0.5−2 h; c: 2−24 h) and $C_{19}H_{26}N_5O_6Br$ in bromination (d: 0−0.5 h; e: 0.5−2 h; f: 2−24 h).

−0.22 to −0.06) of formulas formed in other oxidation processes were observed. Notably, a significantly increased DBE of the formed formulas was observed (Figure S6). Meanwhile, DBE/O values that were inversely related to with the decreased numbers of C═O bonds, and DBE-O values representing the C═C unsaturation by excluding all of the possible C═O bonds decreased. These indicated the formation of C═O bonds (e.g., aldehyde, ketone, and carboxylic acid) in ozonation. According to the KMD ($CH_2$) and KMD (CO) plots (Figure S10), the formed formulas contained higher levels of C═O moieties than the abated formulas, implying the transformation of $CH_2$ moieties to possible carbonyl moieties during ozonation. Meanwhile, the $\overline{OS_c}$ of the formed formulas dominated by CHON molecules substantially increased, the KMD ($NH_2$) and KMD (NOO) indicated the possible transformation of amine to nitro moieties.

A total of 1104 formulas were formed by permanganate oxidation. CHO, CHON, CHOS, and CHONS molecules accounted for 9.1, 39.3, 14.4, and 37.2% of the total formulas, respectively (Figure S9). Substantially larger amounts of CHOS molecules in the aliphatic/peptide-like and carbohydrate-like regions were observed upon permanganate oxidation than other processes. The pronounced formation of CHONS molecules was probably related to the sulfur-containing amino acids/peptides in AOM. It is likely that permanganate preferentially reacted with the amine moieties.[54] Like ozonation, KMD plots revealed the possible transformation of $CH_2$ and $NH_2$ groups to the corresponding carbonyl and nitro moieties (Figure S10).

The $AI_{mod}$ values of formed formulas were significantly lower than those of the abated formulas in the oxidation processes, and permanganate oxidation induced the most pronounced decrease. Meanwhile, significantly elevated $\overline{OS_c}$ was observed in the formed formulas than abated formulas, and ozonation induced the highest level of increase among the five oxidation processes.

**Molecular Transformation Pathways.** To explore the transformation pathways in the five oxidation processes, the mass difference network analysis was conducted based on the reactions summarized in Table S4. The number of identified precursor-product pairs is shown in Figure 5. A total of 3211, 3256, 2935, 4349, and 2671 precursor-product pairs were tentatively identified in chlorination, bromination, chloramination, ozonation, and permanganate oxidation, respectively. Not surprisingly, oxygen transfer (e.g., addition of oxygen atoms, hydroxylation) was the most pronounced transformation pathway (Table S7), elevating the O/C and $\overline{OS_c}$


https://doi.org/10.1021/acsestwater.4c00855
ACS EST Water 2024, 4, 5890−5901

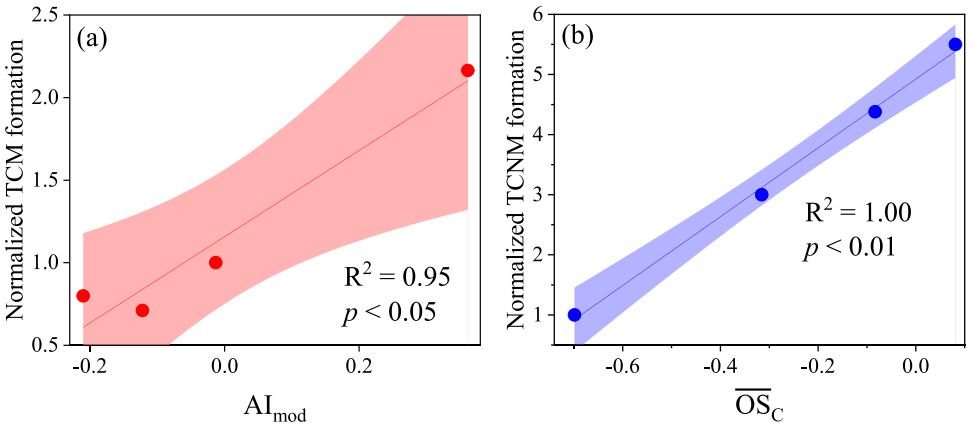


**Figure 7.** Plots of normalized TCM formation vs $AI_{mod}$ values (a) and normalized TCNM formation vs $\overline{OS}_c$ values (b). Data on TCM and TCNM formation were collected from the literature.[34,44,54]

values in oxidized AOM. Besides, oxidative dehydrogenation (e.g., quinone formation from phenols) accounted for approximately 11.9−20.4% of the total identified transformation pathways. Other pathways, such as deamination, dealkylation, decarboxylation, and halogen substitution/addition, existed.

The reaction pathways of assigned formulas containing 19 carbon atoms in chlorination are illustrated in Figure S11. C19 molecules, which were one of the most abundant abated formulas in oxidation processes, were selected. In chlorination, oxygen transfer and oxidative dehydrogenation accounted for 42.5−45.5% of the total identified precursor-product pairs (Figure 5), implying their important roles in altering the molecular characteristics of AOM. Chlorine substitution and addition pathways were relatively minor (7.0−10.3%) (Table S7). The contribution of chlorine substitution to chlorine-containing formulas formed from AOM was more pronounced than that from SR NOM. For example, the numbers of identified precursor-product pairs of chlorine substitution were 4.2−5.4 times as high as those of chlorine addition, which could be ascribed to the lower unsaturation degree of AOM than that of NOM. To reveal formation pathways of most abundant chlorine-containing formula (e.g., $C_{17}H_{23}N_4O_8Cl$), potential reactions at different times (i.e., 0.5, 2, and 24 h) are illustrated in Figure 6. A series of reactions, including oxidation, deamination, dealkylation, and decarboxylation during the first 2 h of chlorination, led to the formation of $C_{17}H_{22}N_4O_7$, $C_{17}H_{24}N_4O_7$, and $C_{17}H_{24}N_4O_8$. These three formulas served as precursors of $C_{17}H_{23}N_4O_8Cl$ via pathways of chlorine substitution/addition.

In bromination, the fraction of each reaction over the total pathways was comparable to chlorination (Figures 5 and S12). Oxygen transfer and oxidative dehydrogenation pathways were also the most pronounced pathways for C19 formulas abated. With prolonged bromination time, an increase in bromine substitution/addition was observed. For example, the percentages of bromine substitution/addition in total reaction pathways were 1.3, 6.0, and 8.0% at times of 0.5, 2, and 24 h, respectively. Akin to chlorination, bromine substitution/addition pathways were minor, agreeing with a previous study that the electrophilic halogen substitution pathway accounts for <10−20% in bromination of NOM extracts.[20] The numbers of bromine substitution pathways were 2.7−2.8 times as high as bromine addition. Similar to the formation of $C_{17}H_{23}N_4O_8Cl$, a series of reactions resulted in the formation of $C_{19}H_{27}N_5O_6$ and $C_{20}H_{27}N_5O_8$, which further led to the formation of $C_{19}H_{26}N_5O_6Br$ via bromine substitution (Figure 6).

Compared with chlorine/bromine, halogenation (e.g., halogen addition and substitution) pathways only accounted for 2.1% of the total identified reactions for AOM treated by chloramine, while 49.0% of the total reactions were ascribed to oxygen transfer and oxidative dehydrogenation pathways (Figure 5). Approximately 45.3% of the assigned formulas with 19 carbon atoms were removed via oxygen transfer and oxidative dehydrogenation pathways (Figure S13).

Not surprisingly, the numbers of precursor-product pairs in ozonation were 1780 and 518 based on the reactions of oxygen transfer and oxidative dehydrogenation, respectively, accounting for >50% of the total identified reaction pathways (Figure 5). Notably, the transformations of methyl to carbonyl moieties and amine to nitro moieties were involved in the oxygen transfer pathways. Besides, the numbers of identified deamination and dealkylation pathways in ozonation were also higher than those in the other oxidation processes (Figure S14).

In permanganate oxidation, the numbers of identified precursor-product pairs of oxygen transfer and oxidative dehydrogenation were 985 and 351, respectively (Figure S15). This agreed well with the less pronounced effect of permanganate on the molecular characteristics (e.g., $\overline{OS}_c$ and O/C values) of AOM as described above.

**Implications to the Formation of DBPs.** Based on the data from FT-ICR MS analyses, attempts to determine the relationships between AOM molecular parameters and DBP formation upon the downstream chlorination process have been made. The data on the formation of selected DBPs [e.g., chloroform (TCM) and trichloronitromethane (TCNM)] were collected from the literature,[34,44,54] which are summarized in Tables S8 and S9. Figure 7 shows the relationships between the normalized DBP (e.g., TCM and TCNM) formation and molecular parameters (i.e., $AI_{mod}$ and $\overline{OS}_c$). Both ozone and permanganate treatment decreased the TCM yields.[34] A positive relationship was observed between the $AI_{mod}$ values and the TCM yields (Figure 7a). As both ozonation and permanganate oxidation substantially decreased the $AI_{mod}$ values of AOM, the formation of TCM from aromatic precursors decreased with the oxidation process with a more pronounced reduction in ozonation. However, as summarized


https://doi.org/10.1021/acsestwater.4c00855
ACS EST Water 2024, 4, 5890−5901

in Table S9, the TCNM yields from AOM during chlorination increased by 3.4 and 2.0 times upon preozonation and permanganate treatment, respectively. It is likely that amine was transformed into nitro moieties, leading to the increased formation of TCNM in postchlorination. TCNM yields correlated well with $\overline{OS_c}$ values (Figure 7b). Further, it was found that the $\overline{OS_c}$ values of precursors subject to halogen substitution/addition were significantly higher than those of the total abated formulas in chlorination and bromination (Figure S16), indicating that the high $\overline{OS_c}$ could facilitate the halogenation pathways for the formation of oxygen-rich halogenated byproducts. Our findings indicate that oxidative treatment of AOM may decrease the formation of TCNM at the expense of elevating TCNM formation in the subsequent chlorine disinfection. However, halonitromethanes are significantly more cytotoxic and genotoxic than regulated trihalomethanes.[55] From the drinking water safety point of view, reduction of AOM concentration by advanced treatment processes (e.g., biofiltration) and optimization of oxidation processes prior to chlorine disinfection to reduce drinking water toxicity in the HAB events may be addressed in the future.

## CONCLUSIONS

Oxidative treatment using chlorine, bromine, chloramine, ozone, and permanganate changed the molecular characteristics of AOM, thereby increasing chemodiversity. Decreased $AI_{mod}$ and increased $\overline{OS_c}$ were observed. The elevation of $\overline{OS_c}$ correlated with the reduction potential of the oxidants (i.e., ozone > chlorine ≈ bromine > permanganate > chloramine). Oxygen addition and oxidative dehydrogenation pathways were major pathways for the oxidation of AOM. Yet, halogen substitution/addition pathways were relatively minor, even for chlorination/bromination of AOM. As compounds with high aromaticity and low $\overline{OS_c}$ were found to be reactive toward chlorine, oxidative treatment on AOM could decrease its reactivity in postchlorination, which decreased the formation of halogenated DBPs (e.g., TCM) from aromatic moieties. Nevertheless, the oxygen addition to the AOM structure in the oxidation process (especially ozonation) can favor the formation of oxygen-rich DBPs (e.g., TCNM) in the subsequent chlorination.

## ASSOCIATED CONTENT

### Supporting Information

The Supporting Information is available free of charge at https://pubs.acs.org/doi/10.1021/acsestwater.4c00855.

Additional details of chemicals, methods, molecular characteristics of AOM, van Krevelen diagram, and Mass network analyses (PDF)

## AUTHOR INFORMATION


### Corresponding Authors

**Chao Liu** − *Key Laboratory of Drinking Water Science and Technology, Research Center for Eco-Environmental Sciences, Chinese Academy of Sciences, Beijing 100085, China; Department of Environmental Engineering and Earth Sciences, Clemson University, Anderson, South Carolina 29625, United States; University of Chinese Academy of Sciences, Beijing 100049, China;* orcid.org/0000-0002-2954-3426; Email: chaoliu@rcees.ac.cn

**Tanju Karanfil** − *Department of Environmental Engineering and Earth Sciences, Clemson University, Anderson, South Carolina 29625, United States;* orcid.org/0000-0003-0986-5628; Email: tkaranf@clemson.edu

### Authors

**Hang Liu** − *Key Laboratory of Drinking Water Science and Technology, Research Center for Eco-Environmental Sciences, Chinese Academy of Sciences, Beijing 100085, China*

**Chengzhi Hu** − *Key Laboratory of Drinking Water Science and Technology, Research Center for Eco-Environmental Sciences, Chinese Academy of Sciences, Beijing 100085, China; University of Chinese Academy of Sciences, Beijing 100049, China;* orcid.org/0000-0001-9898-835X

**Alex T. Chow** − *Department of Earth and Environmental Sciences, Faculty of Science, The Chinese University of Hong Kong, Hong Kong SAR 999077, China;* orcid.org/0000-0001-7441-8934

Complete contact information is available at: https://pubs.acs.org/10.1021/acsestwater.4c00855


### Author Contributions

CRediT: **Chao Liu** conceptualization, data curation, investigation, writing - original draft, writing - review & editing; **Hang Liu** formal analysis, visualization, writing - original draft; **Chengzhi Hu** writing - review & editing; **Alex Tat-Shing Chow** EMSL project leader, writing - review & editing; **Tanju Karanfil** resources, writing - review & editing.

### Notes

The authors declare no competing financial interest.

## ACKNOWLEDGMENTS

This study was funded, in part, by the National Natural Science Foundation of China (Project Nos. 52388101 and 52370019), the National Key Research and Development Program of China (Project No. 2023YFC3207805), the US Environmental Protection Agency (National Priorities: Water Scarcity & Drought, Grant No: R835864), and the Environmental Molecular Sciences Laboratory (EMSL) project (No: 50118). Nevertheless, the manuscript has not been subjected to a policy review of the funding agency and therefore does not necessarily reflect the agency's views. The authors would like to thank Nikola Tolić and Rosalie Chu at the EMSL of the Pacific Northwest National Laboratory for the FT-ICR MS measurement. We thank Dong Cao for sharing the SR NOM data and the kind help on the FT-ICR MS data analyses.

## REFERENCES

(1) Hou, X.; Feng, L.; Dai, Y.; Hu, C.; Gibson, L.; Tang, J.; Lee, Z.; Wang, Y.; Cai, X.; Liu, J.; Zheng, Y.; Zheng, C. Global mapping reveals increase in lacustrine algal blooms over the past decade. *Nat. Geosci.* **2022**, *15* (2), 130−134.

(2) Huisman, J.; Codd, G. A.; Paerl, H. W.; Ibelings, B. W.; Verspagen, J. M. H.; Visser, P. M. Cyanobacterial blooms. *Nat. Rev. Microbiol.* **2018**, *16* (8), 471−483.

(3) Ho, J. C.; Michalak, A. M.; Pahlevan, N. Widespread global increase in intense lake phytoplankton blooms since the 1980s. *Nature* **2019**, *574* (7780), 667−670.

(4) Chapra, S. C.; Boehlert, B.; Fant, C.; Bierman, V. J.; Henderson, J.; Mills, D.; Mas, D. M. L.; Rennels, L.; Jantarasami, L.; Martinich, J.; Strzepek, K. M.; Paerl, H. W. Climate Change Impacts on Harmful Algal Blooms in U.S. Freshwaters: A Screening-Level Assessment. *Environ. Sci. Technol.* **2017**, *51* (16), 8933−8943.

(5) Tsai, K.-P.; Chow, A. T. Growing Algae Alter Spectroscopic Characteristics and Chlorine Reactivity of Dissolved Organic Matter from Thermally-Altered Forest Litters. *Environ. Sci. Technol.* **2016**, *50* (15), 7991−8000.
(6) Liu, C.; Ersan, M. S.; Wagner, E.; Plewa, M. J.; Amy, G.; Karanfil, T. Toxicity of chlorinated algal-impacted waters: Formation of disinfection byproducts vs. reduction of cyanotoxins. *Water Res.* **2020**, *184*, No. 116145.
(7) Yang, M.; Yu, J.; Li, Z.; Guo, Z.; Burch, M.; Lin, T.-F. Taihu Lake Not to Blame for Wuxi's Woes. *Science* **2008**, *319* (5860), 158.
(8) Li, L.; Gao, N.; Deng, Y.; Yao, J.; Zhang, K. Characterization of intracellular & extracellular algae organic matters (AOM) of Microcystic aeruginosa and formation of AOM-associated disinfection byproducts and odor & taste compounds. *Water Res.* **2012**, *46* (4), 1233−1240.
(9) Qi, J.; Lan, H.; Liu, R.; Miao, S.; Liu, H.; Qu, J. Prechlorination of algae-laden water: The effects of transportation time on cell integrity, algal organic matter release, and chlorinated disinfection byproduct formation. *Water Res.* **2016**, *102*, 221−228.
(10) Henderson, R.; Parsons, S. A.; Jefferson, B. The impact of algal properties and pre-oxidation on solid−liquid separation of algae. *Water Res.* **2008**, *42* (8−9), 1827−1845.
(11) Qi, J.; Lan, H. C.; Miao, S. Y.; Xu, Q.; Liu, R. P.; Liu, H. J.; Qu, J. H. KMnO4-Fe(II) pretreatment to enhance *Microcystis aeruginosa* removal by aluminum coagulation: Does it work after long distance transportation? *Water Res.* **2016**, *88*, 127−134.
(12) Lin, J.-L.; Hua, L.-C.; Wu, Y.; Huang, C. Pretreatment of algae-laden and manganese-containing waters by oxidation-assisted coagulation: Effects of oxidation on algal cell viability and manganese precipitation. *Water Res.* **2016**, *89*, 261−269.
(13) Chen, J.-J.; Yeh, H.-H. The mechanisms of potassium permanganate on algae removal. *Water Res.* **2005**, *39* (18), 4420−4428.
(14) Plummer, J. D.; Edzwald, J. K. Effects of chlorine and ozone on algal cell properties and removal of algae by coagulation. *J. Water Supply: Res. Technol.–AQUA* **2002**, *51* (6), 307−318.
(15) Xie, P.; Ma, J.; Fang, J.; Guan, Y.; Yue, S.; Li, X.; Chen, L. Comparison of Permanganate Preoxidation and Preozonation on Algae Containing Water: Cell Integrity, Characteristics, and Chlorinated Disinfection Byproduct Formation. *Environ. Sci. Technol.* **2013**, *47* (24), 14051−14061.
(16) Fang, J.; Yang, X.; Ma, J.; Shang, C.; Zhao, Q. Characterization of algal organic matter and formation of DBPs from chlor(am)ination. *Water Res.* **2010**, *44* (20), 5897−5906.
(17) Her, N.; Amy, G.; Park, H.-R.; Song, M. Characterizing algogenic organic matter (AOM) and evaluating associated NF membrane fouling. *Water Res.* **2004**, *38* (6), 1427−1438.
(18) Hua, L.-C.; Lin, J.-L.; Syue, M.-Y.; Huang, C.; Chen, P.-C. Optical properties of algogenic organic matter within the growth period of Chlorella sp. and predicting their disinfection by-product formation. *Sci. Total Environ.* **2018**, *621*, 1467−1474.
(19) Leenheer, J. A.; Croué, J.-P. Peer Reviewed: Characterizing Aquatic Dissolved Organic Matter. *Environ. Sci. Technol.* **2003**, *37* (1), 18A−26A.
(20) Criquet, J.; Rodriguez, E. M.; Allard, S.; Wellauer, S.; Salhi, E.; Joll, C. A.; von Gunten, U. Reaction of bromine and chlorine with phenolic compounds and natural organic matter extracts − Electrophilic aromatic substitution and oxidation. *Water Res.* **2015**, *85*, 476−486.
(21) Liu, C.; Ersan, M. S.; Plewa, M. J.; Amy, G.; Karanfil, T. Formation of regulated and unregulated disinfection byproducts during chlorination of algal organic matter extracted from freshwater and marine algae. *Water Res.* **2018**, *142*, 313−324.
(22) Liu, C.; Ersan, M. S.; Plewa, M. J.; Amy, G.; Karanfil, T. Formation of iodinated trihalomethanes and noniodinated disinfection byproducts during chloramination of algal organic matter extracted from *Microcystis aeruginosa*. *Water Res.* **2019**, *162*, 115−126.
(23) Minakata, D.; von Gunten, U. Predicting Transformation Products during Aqueous Oxidation Processes: Current State and Outlook. *Environ. Sci. Technol.* **2023**, *57* (47), 18410−18419.
(24) Deborde, M.; von Gunten, U. Reactions of chlorine with inorganic and organic compounds during water treatment - Kinetics and mechanisms: A critical review. *Water Res.* **2008**, *42* (1−2), 13−51.
(25) Liu, C.; Shin, Y.-H.; Wei, X.; Ersan, M. S.; Wagner, E.; Plewa, M. J.; Amy, G.; Karanfil, T. Preferential Halogenation of Algal Organic Matter by Iodine over Chlorine and Bromine: Formation of Disinfection Byproducts and Correlation with Toxicity of Disinfected Waters. *Environ. Sci. Technol.* **2022**, *56* (2), 1244−1256.
(26) Zhang, H.; Zhang, Y.; Shi, Q.; Hu, J.; Chu, M.; Yu, J.; Yang, M. Study on Transformation of Natural Organic Matter in Source Water during Chlorination and Its Chlorinated Products using Ultrahigh Resolution Mass Spectrometry. *Environ. Sci. Technol.* **2012**, *46* (8), 4396−4402.
(27) Zhang, H.; Zhang, Y.; Shi, Q.; Zheng, H.; Yang, M. Characterization of Unknown Brominated Disinfection Byproducts during Chlorination Using Ultrahigh Resolution Mass Spectrometry. *Environ. Sci. Technol.* **2014**, *48* (6), 3112−3119.
(28) Niu, X.-Z.; Harir, M.; Schmitt-Kopplin, P.; Croué, J.-P. Characterisation of dissolved organic matter using Fourier-transform ion cyclotron resonance mass spectrometry: Type-specific unique signatures and implications for reactivity. *Sci. Total Environ.* **2018**, *644*, 68−76.
(29) Ruan, X.; Xiang, Y.; Shang, C.; Cheng, S.; Liu, J.; Hao, Z.; Yang, X. Molecular characterization of transformation and halogenation of natural organic matter during the UV/chlorine AOP using FT-ICR mass spectrometry. *Journal of Environ. Sci.* **2021**, *102*, 24−36.
(30) Hu, W.; Niu, X.-Z.; Chen, H.; Ye, B.; Liang, J.-K.; Guan, Y.-T.; Wu, Q.-Y. Molecular insight of dissolved organic matter and chlorinated disinfection by-products in reclaimed water during chlorination with permanganate preoxidation. *Chemosphere* **2024**, *349*, No. 140807.
(31) Wu, Y.; Sheng, D.; Wu, Y.; Sun, J.; Bu, L.; Zhu, S.; Zhou, S. Molecular insights into formation of nitrogenous disinfection byproducts from algal organic matter in UV-LEDs/chlorine process based on FT-ICR analysis. *Sci. Total Environ.* **2022**, *812*, No. 152457.
(32) Li, T.; Shang, C.; Xiang, Y.; Yin, R.; Pan, Y.; Fan, M.; Yang, X. ClO2 pre-oxidation changes dissolved organic matter at the molecular level and reduces chloro-organic byproducts and toxicity of water treated by the UV/chlorine process. *Water Res.* **2022**, *216*, No. 118341.
(33) Gonsior, M.; Powers, L. C.; Williams, E.; Place, A.; Chen, F.; Ruf, A.; Hertkorn, N.; Schmitt-Kopplin, P. The chemodiversity of algal dissolved organic matter from lysed *Microcystis aeruginosa* cells and its ability to form disinfection by-products during chlorination. *Water Res.* **2019**, *155*, 300−309.
(34) Wu, Y.; Bu, L.; Zhu, S.; Chen, F.; Li, T.; Zhou, S.; Shi, Z. Molecular transformation of algal organic matter during sequential ozonation-chlorination: Role of pre-ozonation and properties of chlorinated disinfection byproducts. *Water Res.* **2022**, *223*, No. 119008.
(35) Dittmar, T.; Koch, B.; Hertkorn, N.; Kattner, G. A simple and efficient method for the solid-phase extraction of dissolved organic matter (SPE-DOM) from seawater. *Limnol. Oceanogr.: Methods* **2008**, *6* (6), 230−235.
(36) Chen, H.; Tsai, K.-P.; Liu, Y.; Tolić, N.; Burton, S. D.; Chu, R.; Karanfil, T.; Chow, A. T. Characterization of Dissolved Organic Matter from Wildfire-induced *Microcystis aeruginosa* Blooms controlled by Copper Sulfate as Disinfection Byproduct Precursors Using APPI(−) and ESI(−) FT-ICR MS. *Water Res.* **2021**, *189*, No. 116640.
(37) Chen, H.; Ersan, M. S.; Tolić, N.; Chu, R. K.; Karanfil, T.; Chow, A. T. Chemical characterization of dissolved organic matter as disinfection byproduct precursors by UV/fluorescence and ESI FT-ICR MS after smoldering combustion of leaf needles and woody trunks of pine (Pinus jeffreyi). *Water Res.* **2022**, *209*, No. 117962.


https://doi.org/10.1021/acsestwater.4c00855
*ACS EST Water* 2024, 4, 5890−5901

(38) Hao, Z.; Yin, Y.; Cao, D.; Liu, J. Probing and Comparing the Photobromination and Photoiodination of Dissolved Organic Matter by Using Ultra-High-Resolution Mass Spectrometry. *Environ. Sci. Technol.* **2017**, *51* (10), 5464−5472.
(39) Hao, Z.; Shi, F.; Cao, D.; Liu, J.; Jiang, G. Freezing-Induced Bromate Reduction by Dissolved Organic Matter and the Formation of Organobromine Compounds. *Environ. Sci. Technol.* **2020**, *54* (3), 1668−1676.
(40) Boye, K.; Noël, V.; Tfaily, M. M.; Bone, S. E.; Williams, K. H.; Bargar, John R.; Fendorf, S. Thermodynamically controlled preservation of organic carbon in floodplains. *Nat. Geosci.* **2017**, *10* (6), 415−419.
(41) Hughey, C. A.; Hendrickson, C. L.; Rodgers, R. P.; Marshall, A. G.; Qian, K. Kendrick Mass Defect Spectrum: A Compact Visual Analysis for Ultrahigh-Resolution Broadband Mass Spectra. *Anal. Chem.* **2001**, *73* (19), 4676−4681.
(42) Ohno, T.; He, Z.; Sleighter, R. L.; Honeycutt, C. W.; Hatcher, P. G. Ultrahigh Resolution Mass Spectrometry and Indicator Species Analysis to Identify Marker Components of Soil- and Plant Biomass-Derived Organic Matter Fractions. *Environ. Sci. Technol.* **2010**, *44* (22), 8594−8600.
(43) Chen, H.; Uzun, H.; Tolić, N.; Chu, R.; Karanfil, T.; Chow, A. T. Molecular Transformation of Dissolved Organic Matter during the Processes of Wildfire, Alum Coagulation, and Disinfection Using ESI(−) and ESI(+) FT-ICR MS. *ACS ES&T Water* **2023**, *3* (8), 2571−2580.
(44) Liu, Y.; Liu, K.; Plewa, M. J.; Karanfil, T.; Liu, C. Formation of regulated and unregulated disinfection byproducts during chlorination and chloramination: Roles of dissolved organic matter type, bromide, and iodide. *J. Environ. Sci.* **2022**, *117*, 151−160.
(45) Kristiana, I.; Gallard, H.; Joll, C.; Croué, J.-P. The formation of halogen-specific TOX from chlorination and chloramination of natural organic matter isolates. *Water Res.* **2009**, *43* (17), 4177−4186.
(46) von Gunten, U. Ozonation of drinking water: Part I. Oxidation kinetics and product formation. *Water Res.* **2003**, *37* (7), 1443−1467.
(47) Laszakovits, J. R.; Somogyi, A.; MacKay, A. A. Chemical Alterations of Dissolved Organic Matter by Permanganate Oxidation. *Environ. Sci. Technol.* **2020**, *54* (6), 3256−3266.
(48) Pourbaix, M. J. N. *Atlas of Electrochemical Equilibria in Aqueous Solutions*; National Association of Corrosion Engineers: Houston, TX, 1974.
(49) Deborde, M.; von Gunten, U. Reactions of chlorine with inorganic and organic compounds during water treatment—Kinetics and mechanisms: A critical review. *Water Res.* **2008**, *42* (1), 13−51.
(50) Kimura, S. Y.; Vu, T. N.; Komaki, Y.; Plewa, M. J.; Mariñas, B. J. Acetonitrile and N-Chloroacetamide Formation from the Reaction of Acetaldehyde and Monochloramine. *Environ. Sci. Technol.* **2015**, *49* (16), 9954−9963.
(51) Wang, D.; He, J.; Ma, J.; Zhang, J.; Strathmann, T. J. Understanding molecular-level reactions between permanganate/ferrate and dissolved effluent organic matter from municipal secondary effluent. *Water Res.* **2023**, *247*, No. 120768.
(52) Sheng, D.; Bu, L.; Zhu, S.; Wu, Y.; Wang, J.; Zhou, S. Organic chloramines formation from algal organic matters: Insights from Fourier transform-ion cyclotron resonance mass spectrometry. *Water Res.* **2021**, *206*, No. 117746.
(53) Li, G.; Tian, C.; Karanfil, T.; Liu, C. Comparative formation of chlorinated and brominated disinfection byproducts from chlorination and bromination of amino acids. *Chemosphere* **2024**, *349*, No. 140985.
(54) Chen, M.; Rholl, C. A.; Persaud, S. L.; Wang, Z.; He, Z.; Parker, K. M. Permanganate preoxidation affects the formation of disinfection byproducts from algal organic matter. *Water Res.* **2023**, *232*, No. 119691.
(55) Wagner, E. D.; Plewa, M. J. CHO cell cytotoxicity and genotoxicity analyses of disinfection by-products: An updated review. *J. Environ. Sci.* **2017**, *58*, 64−76.



https://doi.org/10.1021/acsestwater.4c00855
*ACS EST Water* 2024, 4, 5890−5901